

GaN Lattice Damage and GaN-HEMT Metrology by Cameraless T-Ray Imaging and Time-Domain Spectroscopy

Anis Rahman^{1,*}

¹Applied Research & Photonics, Inc., USA

Abstract: Gallium nitride (GaN) film grown on a silicon substrate has been investigated for high electric field-induced lattice damage via cameraless terahertz (T-ray) imaging technique. In addition, T-ray time-domain spectroscopy (TDS) has been conducted on the same GaN film as a function of depth via nondestructive and noncontact pump-probe technique. This is termed as the deep-level TDS. Further, a pair of GaN high electron mobility transistor (HEMT) dies has been imaged at the channel area where the deep-level TDS has also been conducted. A pristine die has been compared with a similar die that was irradiated with mild nuclear radiation. The channel width measured via T-ray metrology of both dies matches those determined from the optical microscope images. However, T-ray deep-level spectral analysis of both dies reveals that the pristine die's channel structure remains unaffected up to 5.5 THz up to a depth of 3 μm while that of the irradiated die's channel structure's performance is shrunk to 4.2 THz to the same depth of 3 μm . Details of data and analysis have been discussed. The technique may be deployed to other similar systems and devices.

Keywords: T-ray volume imaging, GaN lattice damage, GaN film, GaN HEMT, T-ray deep-level spectroscopy, radiation treatment

1. Introduction

Gallium nitride (GaN) transistors are a type of semiconductor device that has gained significant importance in recent years due to their superior performance and potential for various applications. GaN is a compound semiconductor that could emerge as an alternative to silicon for high-power electronics and high-frequency applications. GaN transistors, specifically high electron mobility transistors (HEMTs), have several advantages over traditional silicon-based devices, making them attractive for a wide range of applications. GaN has a wide bandgap, high electron mobility, and the ability to withstand high electric fields, which translates into several benefits for transistor applications. These properties enable GaN transistors to operate at higher voltages, higher frequencies, and higher temperatures, compared to silicon-based devices. Additionally, GaN transistors exhibit lower on-resistance, resulting in reduced power losses and improved efficiency [1, 2]. The structural breakdown in high-power GaN-on-GaN p-n diode devices due to stress has been reported [3, 4]. Structural damage may also evolve in GaN crystals due to grinding and polishing processes [5]. A review has been provided by Karami and Haziq et al. [6, 7].

Nonetheless, GaN-based HEMTs offer the following notable advantages for high-frequency applications [8, 9]. One of the key advantages of GaN transistors is their ability to operate at higher frequencies, making them suitable for applications such as radar systems, satellite communications, and 5G wireless networks. The

high electron mobility and saturation velocity of GaN allow for faster switching speeds and higher operating frequencies, enabling more efficient and compact radio frequency systems.

1.1. Power electronics

GaN transistors are useful for the power electronics industry because they enable more efficient and compact power conversion systems [10]. They are particularly well-suited for applications such as power supplies, motor drives, and renewable energy systems. The high breakdown voltage and low on-resistance of GaN transistors allow for higher power densities and reduced cooling requirements, leading to smaller and more efficient power conversion systems.

The GaN transistors offer advantages for applications in space and radiation environments. Space exploration pushes the boundaries of technology, demanding components that can withstand harsh environments unlike anything found on Earth. In this arena, GaN transistors are emerging as a game-changer, offering significant advantages over traditional silicon-based solutions for space and radiation applications [11–15]. One of the most compelling features of GaN transistors for space applications is their superior radiation hardness. Unlike silicon, which degrades in performance when exposed to radiation, GaN exhibits exceptional resilience. This is crucial for satellites and spacecraft orbiting in the harsh environment of space, constantly being bombarded by high-energy particles. GaN transistors can maintain their functionality for extended periods, ensuring reliable operation of critical systems onboard.

Furthermore, GaN transistors boast superior efficiency compared to their silicon counterparts. They operate at higher

*Corresponding author: Anis Rahman, Applied Research & Photonics, Inc., USA. Email: a.rahman@arphotonics.net

frequencies, enabling the development of compact and lightweight power converters. This is a significant advantage for space missions, where every gram counts. Smaller and lighter power converters translate into reduced launch costs and increased payload capacity. Additionally, the higher efficiency of GaN transistors minimizes heat generation, a critical factor in the thermally constrained environment of spacecraft.

1.2. Energy efficiency and sustainability

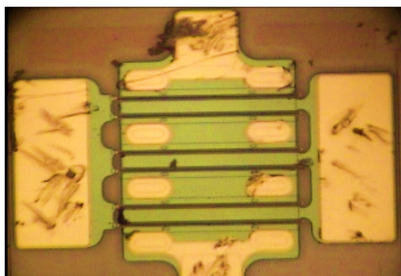
GaN transistors also offer significant advantages in terms of power density. They can handle larger currents and voltages compared to silicon transistors of similar sizes. This translates to the ability to design more powerful and compact electronics for space applications. For instance, GaN transistors can be used in high-power radar systems, electric propulsion systems for spacecrafts, and efficient solar power conversion units for satellites. The superior efficiency of GaN transistors translates into significant energy savings and reduced environmental impact. By minimizing power losses, GaN-based systems can operate with higher efficiency, resulting in lower energy consumption and reduced greenhouse gas emissions. This makes GaN transistors an attractive choice for sustainable and energy-efficient applications, such as electric vehicles and renewable energy systems. Figure 1 shows an example of a GaN HEMT die that was used for the present investigations.

1.3. Challenges and prospects

Despite the above-mentioned advantages, the widespread adoption of GaN transistors faces challenges related to manufacturing costs, reliability, thermal, and high electric field management. Ongoing research and development efforts are focused on addressing these challenges and further improving the performance and cost-effectiveness of GaN devices. As the demand for energy-efficient and high-performance electronics continues to grow, GaN transistors are poised to play a pivotal role in various industries, including telecommunications, aerospace, automotive, and renewable energy. With their superior material properties and potential for further advancements, GaN transistors represent a significant step forward in the evolution of semiconductor technology.

Another important challenge is that growing GaN boules is a very complex process that involves several advanced techniques to achieve high-quality crystals suitable for transistors, including high-power and high-frequency electronic devices. Techniques like Hydride Vapor Phase Epitaxy (HVPE), ammonothermal growth, melt-solution growth, and Na-flux method each offer limited success and challenges. The largest GaN boules produced today are typically grown using the HVPE method. This method has enabled the production of GaN substrates up to 150 mm in diameter, with

Figure 1
A GaN HEMT die, mildly treated with radiation



thicknesses of 2.6, 5.8, and 6.3 mm only. As such, mass production of GaN-based integrated circuit (IC) is still not economically viable. The challenges collectively contribute to the complexity and cost of GaN-based IC manufacturing, limiting its widespread adoption despite its superior electrical properties in many applications.

In this work, we discuss the lattice damage of GaN film under high electric field stress via high-resolution T-ray volume imaging. The T-ray time-domain deep-level spectral characterization of the GaN film is also briefly discussed. In addition, transistors made from GaN are imaged. Two GaN transistors, one is as-manufactured, and the other one treated with mild nuclear radiation, have been reported with their T-ray time-domain deep-level spectral analysis.

1.4. Review of T-ray methodologies

1.4.1. High-resolution cameraless T-ray volume imaging

High-resolution cameraless T-ray (terahertz radiation) volume imaging is an innovative technique that leverages the unique properties of terahertz radiation to achieve detailed, non-invasive imaging of various materials [16]. T-ray, also known as the far-IR, occupies the frequency range between infrared light and microwaves. Recently, T-ray techniques garnered significant interest due to T-ray's non-ionizing nature and ability to penetrate various non-metallic materials. High-resolution cameraless T-ray volume imaging utilizes these properties to create detailed three-dimensional images, making it a valuable tool in the field of materials characterization. Cameraless T-ray imaging involves the probing of a sample using a nanoscanner without the use of traditional camera systems. Key components include a T-ray source, suitable measurement system, image generation, analysis, and quantification. Readers are encouraged to review refs 2 and 3 for the details of the technique.

1.4.2. T-ray time-domain deep-level spectroscopy

T-ray time-domain deep-level spectroscopy is a cutting-edge technique that leverages the unique properties of T-ray to probe deep-level properties in materials. T-ray time-domain spectroscopy (TDS), highlighting its advantages and potential challenges, has been reviewed by Koch et al. [17]; however, a deep-level investigation has been conducted for the present work. Additionally, Auston switch-based terahertz generation's [18] limitations have been overcome by the dendrimer dipole excitation source [19] which has been used in the present work. The deep-level T-ray TDS allows probing not only the surface of a specimen but also at deeper levels as needed.

2. Experimental

Figure 2 exhibits the TN3DI system (Applied Research & Photonics, Inc., Harrisburg, PA) that was deployed for the present investigations. The system is comprised of a main box (A) that houses a continuous wave terahertz source and detection system, a nanoscanner (B) along with a sample holder (C), and a computer system for the operation of the TN3DI and image analysis. The main box (A) is fitted with a vertical positioning stage (D) and an aperture (E) on the front side for controlling the T-ray beam power. It is noted that delicate samples require relatively low-power scan for a sharper image generation. As explained elsewhere [3], image generation is a two-step process. In the first step, the nanoscanner is engaged via the front-end software to scan a user-specified volume of the sample. The reflected intensity signals corresponding to the scanned volume are stored in a matrix termed as the Beer-Lambert reflection matrix (the BLR matrix). The matrix is then subjected to

Figure 2
Photograph of the TN3DI setup: (A) the main box housing the T-ray source and detection system, (B) nanoscanner (X, Y, and Z axes), (C) Sample holder with a sample on it, (D) vertical positioning stage, (E) Aperture

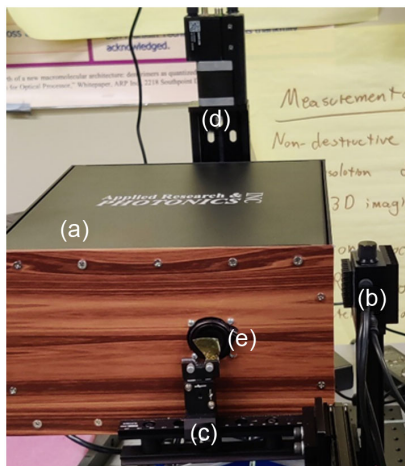
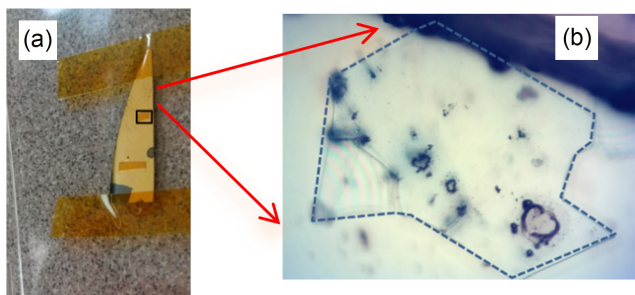


Figure 3
(a) Photographs of the sample as received And (b) area of interest for imaging



an algorithm for image generation and manipulation at the second step; see more details in Rahman [16].

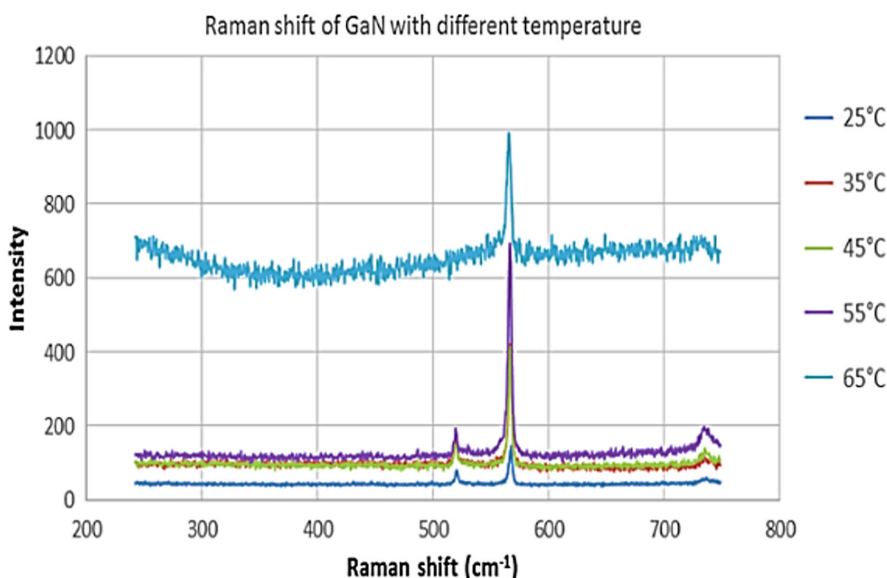
3. Results

3.1. High voltage-induced lattice damage of GaN film

Figure 3(a) exhibits a polycrystalline GaN film grown on silicon substrate. This GaN epi was investigated by ARP's terahertz nanoscanning 3D imager (TN3DI) and time-domain spectrometer. The growth details of the epi are not known at the time of this investigation. However, the common growth process of GaN epitaxial layers on Si wafers typically involves metalorganic chemical vapor deposition. This process has several key steps and considerations which are not a part of the present investigation. The reader is encouraged to consult the work of Schimmel et al. [2] for some details. Here, the as-received sample was previously subjected to a high electric field experiment by the supplier. As such, high field-induced damage might have occurred in its lattice structure. Especially, some areas with black spots are visible under a light microscope (Figure 3(b)); thus, it is suspected that the crystal lattice of the film might have distorted in these areas.

The GaN film is 2 μm thick but no further details were available. However, the available Raman spectra of this sample as depicted in Figure 4 do not provide any information regarding the nature of damage, if any. A slight temperature-dependent shift is observed in the Raman spectra. T-ray is known to be highly sensitive and can penetrate all semiconductors; therefore, it is expected that a combination of T-ray imaging and T-ray TDS will help identify the lattice damage and shed light regarding the nature of damage. Details of cameraless T-ray imaging technique have been described elsewhere [16]. As reported, the technique breaks the wavelength barrier for sub-nanometer resolution imaging with bigger wavelengths such as the T-ray by decoupling the wavelength from image forming mechanism. It is also a nondestructive and noncontact mode probing route.

Figure 4
Raman spectra show prominent peaks at 567.9 cm^{-1} at room temperature (25°C)



3.2. T-ray image analysis of GaN lattice damage

Figure 5 exhibits a 3D view of a small volume ($5\ \mu\text{m} \times 5\ \mu\text{m} \times 2\ \mu\text{m}$) from the top of the GaN film under investigation. The top surface of Figure 5 is reproduced in Figure 6. Here, the undamaged area is identified by regular lattice pattern while the upper area exhibits distorted lattice pattern. The distorted lattice structure (Figure 6) indicates that the GaN crystalline structure of the present sample has been damaged and distorted by the high electric field stress.

Figure 5

A 3D view of $5\ \mu\text{m} \times 5\ \mu\text{m} \times 2\ \mu\text{m}$ volume from the top of the sample. The crystalline area is identified by regular lattice pattern. Damaged areas are also shown as identified by distorted lattice pattern

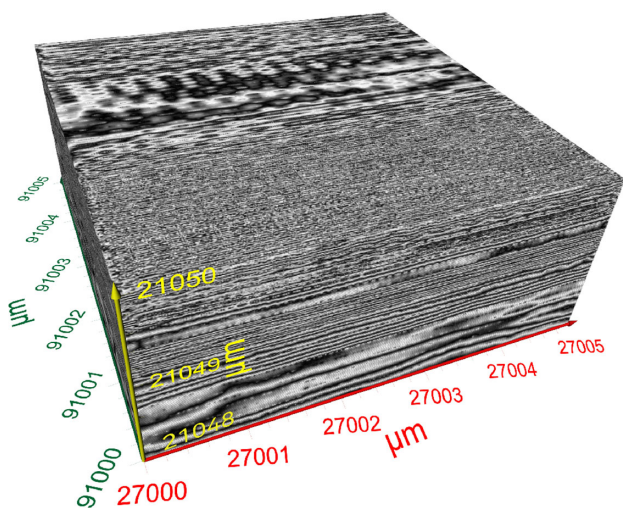
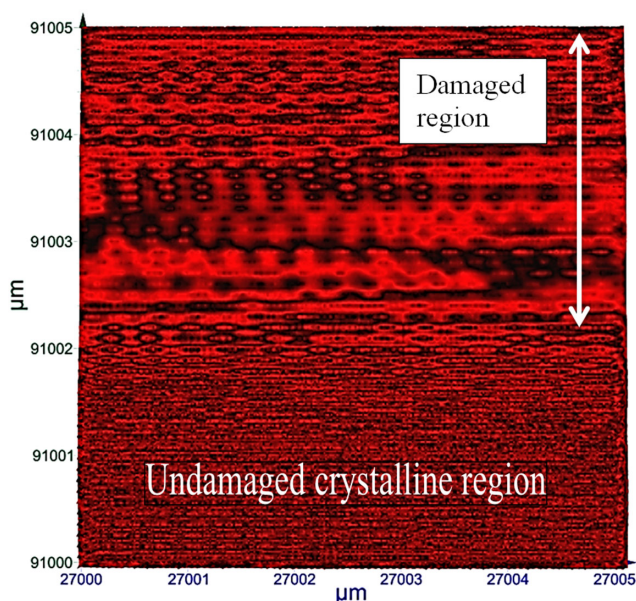


Figure 6

Top surface ($5\ \mu\text{m} \times 5\ \mu\text{m}$) from Figure 3 shows single crystalline area and areas with modified patterns



3.3. T-ray time-domain deep-level spectral analysis of GaN film

T-ray TDS investigation was also conducted on the same GaN sample. Details of terahertz TDS were described elsewhere [8]. The most important aspect of the TDS is the pump-probe detection technique originally proposed by Zewail [20]. The TDS has revolutionized mechanistic investigations of chemical dynamics [9]. As such, the pump-probe spectroscopy is an exemplary ultrafast technique. Here, a coherent beam is divided into two arms of unequal intensity, where one arm is called the pump arm which is used to probe a sample into an electronically and/or vibrationally excited state which is then probed by the second beam to interrogate the change in transmission (or reflection) after a time delay. An advantage here is that the delay time may be adjusted to activate and sense different molecular events [21].

For the present case, the deep-level time-domain signals (aka, interferograms) were acquired as a function of depth, from the surface to up to 2000 nm deep, at a step size of 50 nm. Figure 7 exhibits the depth evolution of the T-ray time-domain interferograms. Two of these time-domain signals were analyzed by Fourier transform technique” one on the surface and one at a depth of $1\ \mu\text{m}$. The computed T-ray absorbance spectra of the GaN film obtained via Fourier transform of the time-domain signals are shown in Figure 8. The absorbance spectrum at the surface of the film (red curve) exhibits a water peak at low frequencies due to ambient moisture while the spectrum at a depth of $1\ \mu\text{m}$ does not exhibit prominent water peak, as indicated by red arrow in Figure 8.

As evident from Figure 8, there are shifts in the peaks between these two spectra, presumably due to the distorted nature of the crystal lattice as seen from the images. The spectra allow a scope of further analysis for better interpretation of the peaks. Figure 9(a) exhibits a volume (3D) image of another area of the same sample showing some details of the GaN layer. Figure 9(b) exhibits two different slices from Figure 9(a) along the YZ plane. Variation of patterns in the layers along the Y-axis is visible.

Figure 10(a) shows a single slice of the YZ plane of Figure 9(a); layers of crystalline area and distorted area are visible here as well. Figure 10(b) displays a graphical analysis of Figure 10(a) along the vertical line. The thickness of the crystalline layers and the distorted layers are plotted on a grayscale. The thickness of the GaN is $\sim 2\ \mu\text{m}$.

Figure 7

Evolution of terahertz time-domain signal (interferogram) as a function of depth from surface to inward. These composite interferograms are the basis of deep-level spectroscopy

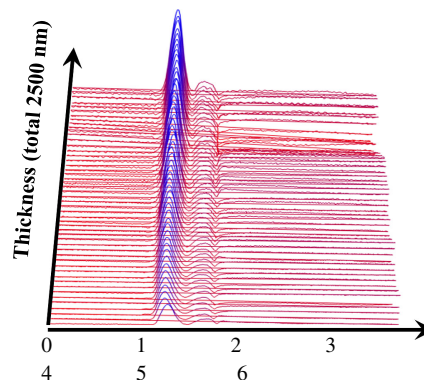
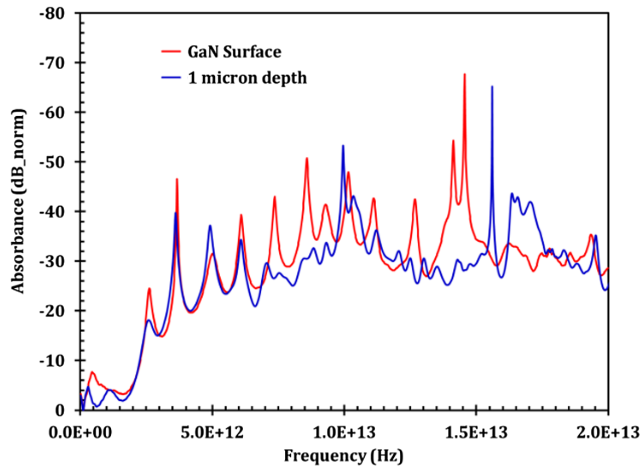


Figure 8

Terahertz absorbance spectra of the GaN sample at the surface (red curve: GaN) and at 1 μm depth from surface. The shifts in the peaks are presumably due to distorted nature as seen in the images. The arrow indicates absorbance peak due to moisture



Other thicknesses of different layers may be quantified from this profile plot of Figure 10(b).

3.4. T-ray metrology of GaN HEMT treated with nuclear radiation

As indicated before, a GaN HEMT is a type of field-effect transistor (FET) that incorporates junctions between two materials with different band gaps (known as a heterojunction) that serve as the channel. Unlike traditional FETs, which rely on a doped region for the channel, HEMTs use this heterojunction to achieve unique characteristics. Two samples of GaN HEMT die were received. One of them was without radiation treatment, and the other one was treated with mild nuclear radiation (Figure 11). Representative imaging results of both are given below. Figure 12 displays a profile along the channel (from Figure 11); the measured channel width is $\sim 8 \mu\text{m}$ at the bottom end. T-ray imaging was conducted on both dies.

3.4.1. T-ray image of unirradiated die

Figure 13(a) exhibits a T-ray image of a pristine GaN HEMT die (not irradiated). The measured channel width via graphical analysis is $\sim 7.97 \mu\text{m}$ Figure 13(b).

3.4.2. T-ray image of irradiated die

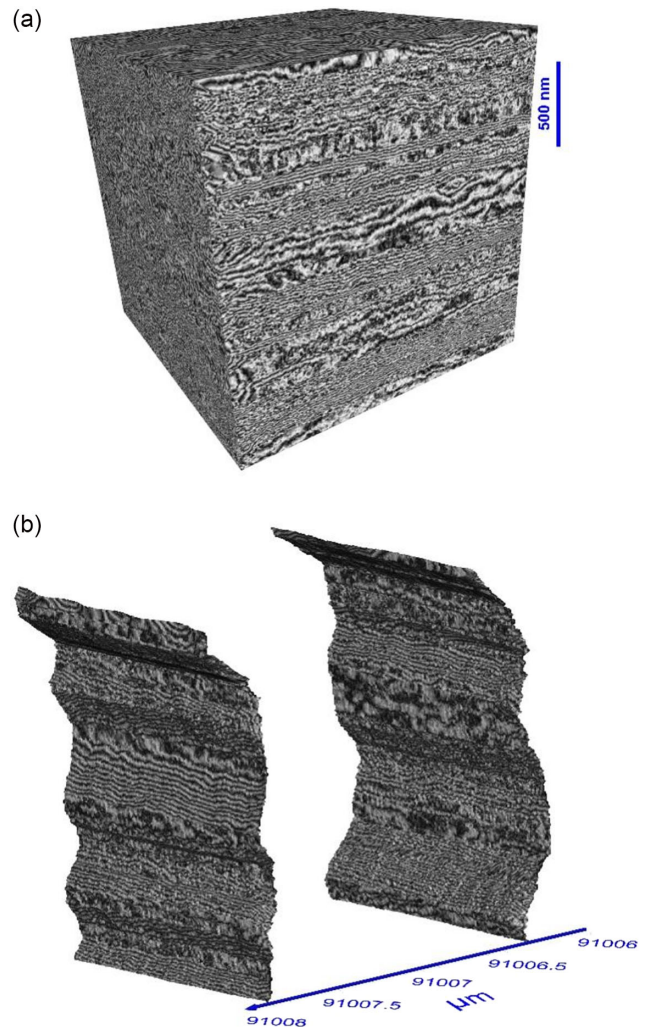
The same quantities for an irradiated die are shown in Figure 14. Here the T-ray image of an irradiated GaN die is shown in Figure 14(a) and (b) shows the measured channel width is $\sim 8.0 \mu\text{m}$.

3.5. Time-domain deep-level spectral analysis of GaN HEMT die

So, why is the depth structure of a HEMT channel important? The depth structure of a HEMT channel is crucial for several reasons, first the formation of 2DEG. The precise depth and composition of the layers in a HEMT structure determine the formation and characteristics of the two-dimensional electron gas (2DEG). The 2DEG is the key feature of HEMTs, allowing for high electron mobility and fast switching speeds, second, the carrier concentration

Figure 9

(a) A volume image of another area of the same sample showing the details of the GaN layer. The thickness of the GaN is $\sim 2 \mu\text{m}$ (see Figure 9). (b) Two single-plane slices from Fig. (a) on the YZ plane. The images represent the actual morphology of the slices at the chosen location along the Y-axis



profile. The depth profile of the carrier concentration is critical for optimizing device performance. Revealed in a study of AlGaIn channel HEMTs, the carrier concentration reaches its maximum at the interface between the barrier and channel layers, typically around 25 nm deep [22]. This concentration profile directly affects the sheet resistance and overall device performance.

In addition, confinement of electrons is influenced by the depth structure. That is, the depth structure influences how well the electrons are confined to the channel region. Proper confinement is essential for maintaining high electron mobility and reducing scattering effects. The following factors also depend on the channel's depth structure.

Control of threshold voltage: The depth and composition of the layers, particularly the barrier layer, affect the threshold voltage of the device. This is crucial for determining whether the HEMT operates in enhanced mode or depletion mode. Minimizing parasitic effects: The depth structure impacts the occurrence of parasitic conduction paths and unwanted carrier generation, which can degrade device performance. Scaling and gate control: The depth structure, especially the gate length and the distance between the gate and the channel, affects the device's ability to be

Figure 10

(a) A single face (YZ plane) of the volume image [Figure 9(a)] is used for graphical analysis. Layers of crystalline area and distorted area are visible. (b) Graphical analysis of (a). The thicknesses of the crystalline layers and the distorted layers are quantified via a grayscale profile plot

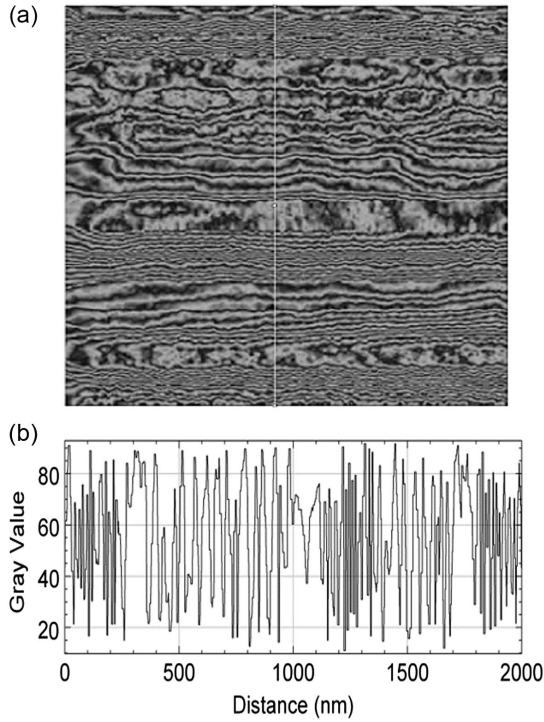
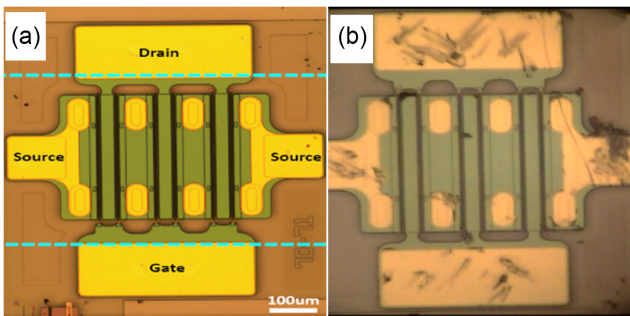


Figure 11

GaN transistor example. (a) As-fabricated die, (b) die irradiated by nuclear radiation (mild dose). Both are from an optical microscope



scaled down and the effectiveness of gate control over the channel. Crystalline quality: The depth structure influences the crystalline quality of the layers, which in turn affects the sheet resistance and overall performance of the device. Studies have shown that improving the crystalline quality of the channel layer can significantly reduce sheet resistance.

By carefully engineering the depth structure of a HEMT channel, manufacturers can optimize the device's performance characteristics, including electron mobility, carrier concentration, threshold voltage, and high-frequency operation capabilities. This

Figure 12

Profile along the channel (from Figure 10) shows the width is $\sim 8 \mu\text{m}$ at the bottom end

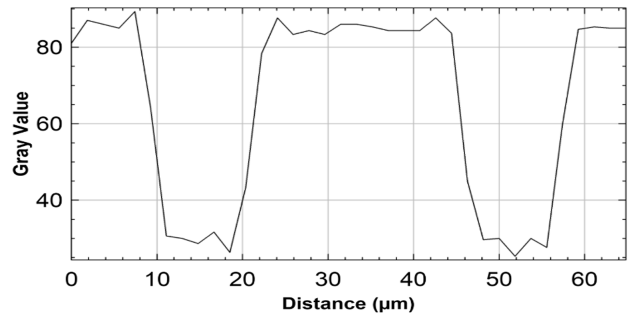
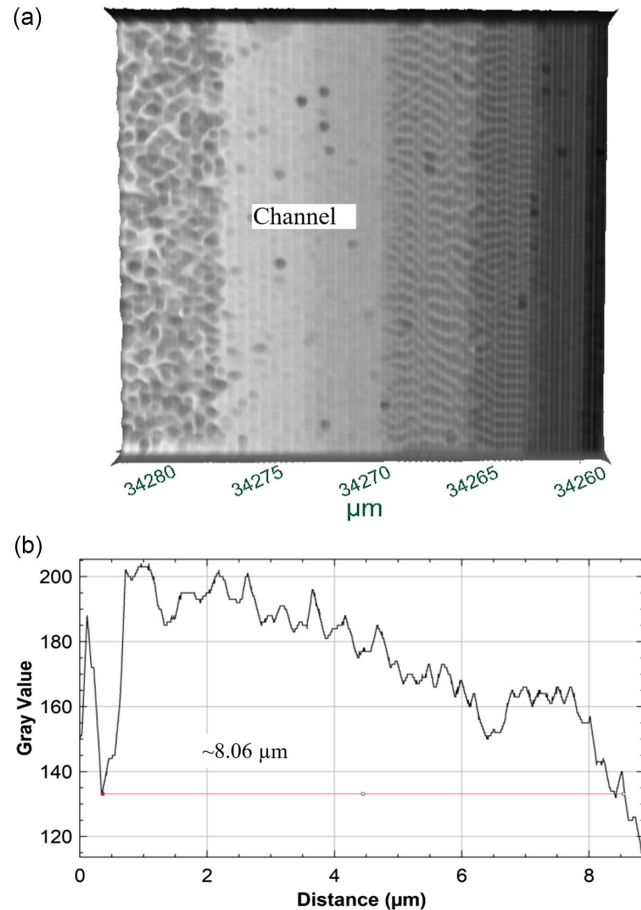


Figure 13

(a) T-ray image of an unirradiated GaN die. (b) Measured channel width is $\sim 8.06 \mu\text{m}$



level of control is what makes HEMTs superior to conventional transistors in many high-frequency and high-power applications. In all cases, the nanostructural properties of the epitaxial GaN film play a crucial role [23–25].

Figure 15 exhibits the absorbance spectra of the pristine HEMT die to a depth of 3 μm at an interval of 1 μm. Figure 16 compares all four spectra in one plot where two regions of frequency dependence are seen. At low frequencies, $< 5.5 \text{ THz}$, all spectra fall on top of each

Figure 14
 (a) T-ray image of an unirradiated GaN die.
 (b) Measured channel width is $\sim 8.0 \mu\text{m}$

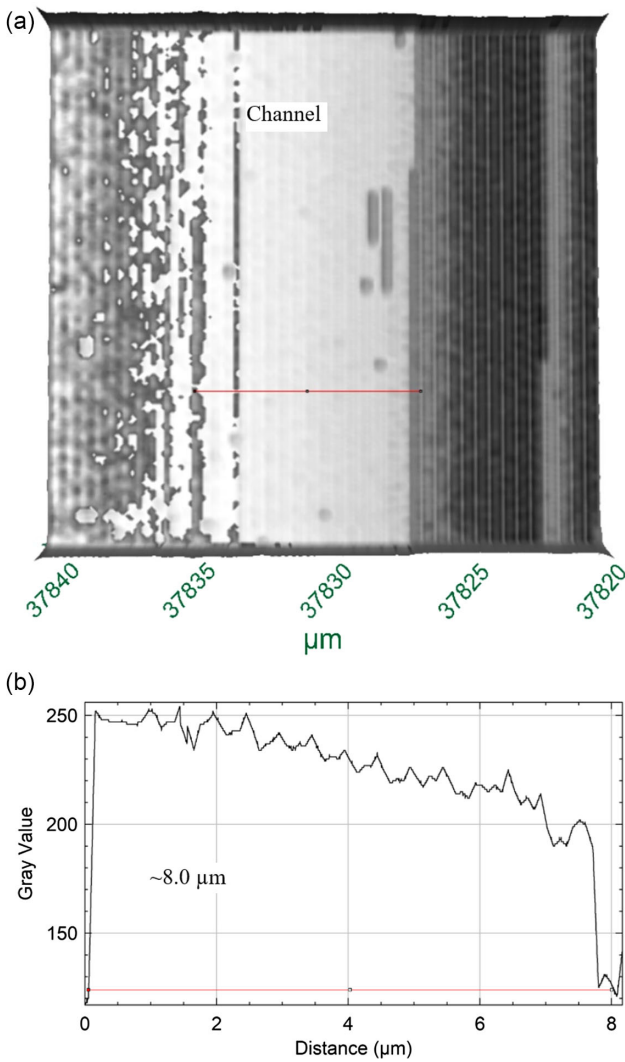


Figure 15
 T-ray absorbance spectra of the pristine die (channel area) as a function of depth, showing the depth-dependent changes from surface to $3 \mu\text{m}$

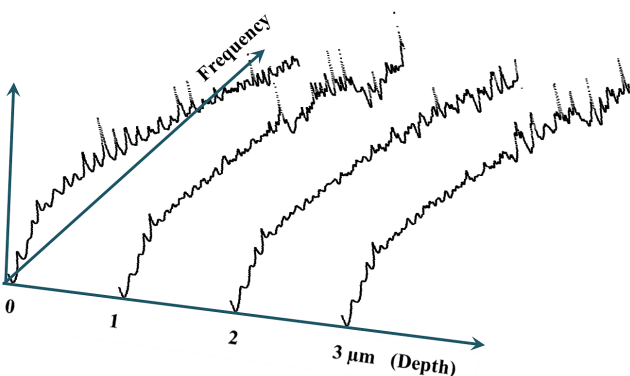


Figure 16
 Comparison of the absorbance spectra of the pristine die channel as a function of depth from surface to $3 \mu\text{m}$

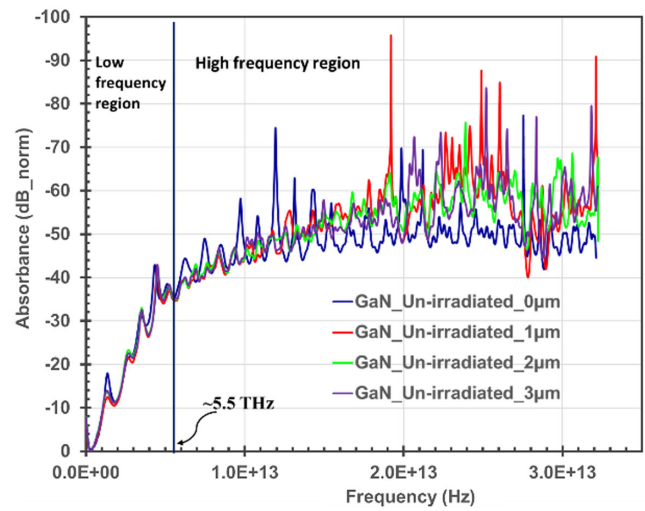
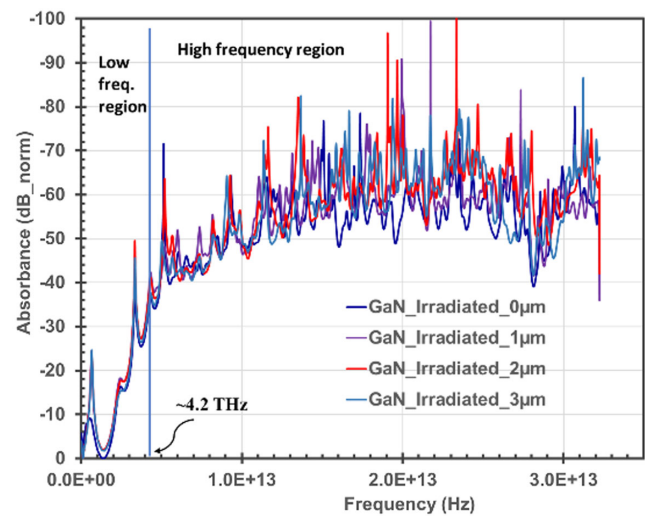


Figure 17
 Comparison of the absorbance spectra of the irradiated die channel as a function of depth from surface to $3 \mu\text{m}$



other, indicating that there is no frequency-dependent change up to the depth of $3 \mu\text{m}$, as shown in Figure 16. At higher frequencies above 5.5 THz , the absorbance peaks exhibit shifts as a function of depth. The absorbance magnitude also varies as a function of depth which is visible above 10 THz .

Figure 17 compares four spectra of the die that was irradiated with mild nuclear radiation (of unknown dose, duration, and other parameters). Here also two regions of frequency dependence seen, however, the low-frequency region has been shrunk to $\sim 4.2 \text{ THz}$, where all spectra fall on top of each other, indicating that there is no significant frequency dependent change in this frequency range up to the depth of $3 \mu\text{m}$. At higher frequencies above 4.2 THz , the absorbance peaks exhibit shifts as a function of depth. The absorbance magnitude also varies as a function of depth which is visible above 10 THz .

4. Discussion on Irradiated vs. Pristine HEMT Die

Based on the very limited information available for the irradiation conditions, a rigorous comparison between the two samples was not possible. Nonetheless, the spectral analysis presented herein demonstrates the capabilities of the technique for this investigation. GaN HEMTs are known to demonstrate significantly higher radiation tolerance compared to their GaAs counterparts. They are expected to be approximately ten times more tolerant of radiation-induced displacement damage. From the deep-level absorbance spectral analysis (Figures 16 and 17), it is seen that at low frequencies the depth dependence is negligible, but at higher frequencies loss factor becomes discernible as a function of depth. Further analysis should produce more information on the channel characteristics of the present GaN HEMT dies. More importantly, the technique may be used to characterize other important channel properties of either GaN or other transistors.

5. Conclusion

In conclusion, the present investigation has demonstrated the effectiveness of T-ray imaging for quantitative measurements of GaN lattice damage and metrology of GaN-based transistors. The high penetration depth and sensitivity of T-ray allowed for nondestructive characterization, providing valuable insights into the material quality and device structure. The ability to detect subtle variations in lattice structure, and identify defects with higher resolution, makes T-ray a powerful tool for optimizing GaN device fabrication and performance. Future research directions could involve correlating T-ray measurements with electrical characterization of devices to establish a more comprehensive understanding of GaN material properties and device behavior. Additionally, the T-ray deep-level absorbance spectral analysis revealed that at low frequencies the depth dependence in the channel region is negligible, but at higher frequencies loss factor becomes significant as the channel depth increases. This provides a means for quantitative assessment of clean signal frequency limit from the current HEMT. Looking forward, the potential of T-ray for monitoring GaN device performance during operation could provide valuable insights into degradation mechanisms and pave the way for the development of more reliable and high-performance GaN electronics.

Ethical Statement

This study does not contain any studies with human or animal subjects performed by the author.

Conflicts of Interest

The author declares that he has no conflicts of interest to this work.

Data Availability Statement

Data are available on request from the corresponding author upon reasonable request.

Author Contribution Statement

Anis Rahman: Conceptualization, Methodology, Validation, Formal analysis, Investigation, Resources, Data curation, Writing – original draft, Writing – review & editing, Visualization, Project administration.

References

- [1] Meneghini, M., Meneghesso, G., & Zanoni, E. (2017). *Power GaN devices: Materials, applications and reliability*. Switzerland: Springer. <https://doi.org/10.1007/978-3-319-43199-4>
- [2] Schimmel, S., Tomida, D., Ishiguro, T., Honda, Y., Chichibu, S. F., & Amano, H. (2023). Temperature field, flow field, and temporal fluctuations thereof in ammonothermal growth of bulk GaN—Transition from dissolution stage to growth stage conditions. *Materials*, 16(5), 2016. <https://doi.org/10.3390/ma16052016>
- [3] Peri, P., Fu, K., Fu, H., Zhao, Y., & Smith, D. J. (2020). Structural breakdown in high power GaN-on-GaN *p-n* diode devices stressed to failure. *Journal of Vacuum Science & Technology A*, 38(6), 063402. <https://doi.org/10.1116/6.0000488>
- [4] Latry, O., Moulitif, N., Joubert, E., & Ndiaye, M. (2022). A time to failure evaluation of AlGaIn/GaN HEMT transistors for RF applications. *e-Prime-Advances in Electrical Engineering, Electronics and Energy*, 2, 100062. <https://doi.org/10.1016/j.prime.2022.100062>
- [5] Li, C., Hu, Y., Wei, Z., Wu, C., Peng, Y., Zhang, F., & Geng, Y. (2024). Damage evolution and removal behaviors of GaN crystals involved in double-grits grinding. *International Journal of Extreme Manufacturing*, 6(2), 025103. <https://doi.org/10.1088/2631-7990/ad207f>
- [6] Karami, K. (2023). *GaN HEMT technology for W-band frequency applications*. PhD Thesis, University of Glasgow.
- [7] Haziq, M., Falina, S., Manaf, A. A., Kawarada, H., & Syamsul, M. (2022). Challenges and opportunities for high-power and high-frequency AlGaIn/GaN high-electron-mobility transistor (HEMT) applications: A review. *Micromachines*, 13(12), 2133. <https://doi.org/10.3390/mi13122133>
- [8] Paz-Martínez, G., Íñiguez-de-la-Torre, I., Artillan, P., Sánchez-Martín, H., García-Sánchez, S., González, T., & Mateos, J. (2024). High-frequency microwave detection with GaN HEMTs in the subthreshold regime. *IEEE Transactions on Microwave Theory and Techniques*, 72(6), 3753–3758. <https://doi.org/10.1109/TMTT.2023.3333418>
- [9] Eastman, L. F., Tilak, V., Kaper, V., Smart, J., Thompson, R., Green, B., . . . , & Prunty, T. (2002). Progress in high-power, high frequency AlGaIn/GaN HEMTs. *Physica Status Solidi (A)*, 194(2), 433–438. [https://doi.org/10.1002/1521-396X\(200212\)194:2<433::AID-PSSA433>3.0.CO;2-R](https://doi.org/10.1002/1521-396X(200212)194:2<433::AID-PSSA433>3.0.CO;2-R)
- [10] Wu, Y. F., Kopolnek, D., Ibbetson, J. P., Parikh, P., Keller, B. P., & Mishra, U. K. (2001). Very-high power density AlGaIn/GaN HEMTs. *IEEE Transactions on Electron Devices*, 48(3), 586–590. <https://doi.org/10.1109/16.906455>
- [11] Sequeira, M. C., Mattei, J. G., Vazquez, H., Djurabekova, F., Nordlund, K., Monnet, I., . . . , & Lorenz, K. (2021). Unravelling the secrets of the resistance of GaN to strongly ionising radiation. *Communications Physics*, 4(1), 51. <https://doi.org/10.1038/s42005-021-00550-2>
- [12] Titov, A. I., Karaseov, P. A., Karabeshkin, K. V., & Struchkov, A. I. (2019). The formation of radiation damage in GaN during successive bombardment by light ions of various energies. *Vacuum*, 173, 109149. <https://doi.org/10.1016/j.vacuum.2019.109149>
- [13] Barber, R., Nguyen, Q., Brockman, J., Gahl, J., & Kwon, J. (2020). Thermal neutron transmutation doping of GaN semiconductors. *Scientific Reports*, 10(1), 16295. <https://doi.org/10.1038/s41598-020-72862-2>
- [14] Pearton, S. J., Aitkaliyeva, A., Xian, M., Ren, F., Khachatryan, A., Ildefonso, A., . . . , & Kim, J. (2021). Review—Radiation damage in wide and ultra-wide bandgap semiconductors.

- ECS Journal of Solid State Science and Technology*, 10(5), 055008. <https://doi.org/10.1149/2162-8777/ABFC23>
- [15] Fleetwood, D. M., Zhang, E. X., Schrimpf, R. D., & Pantelides, S. T. (2022). Radiation effects in AlGaIn/GaN HEMTs. *IEEE Transactions on Nuclear Science*, 69(5), 1105–1119. <https://doi.org/10.1109/TNS.2022.3147143>
- [16] Rahman, A. (2023). T-ray wavelength decoupled imaging and profile mapping of a whole wafer for die sorting and analysis. *Sensors*, 23(7), 3663. <https://doi.org/10.3390/s23073663>
- [17] Koch, M., Mittleman, D. M., Ornik, J., & Castro-Camus, E. (2023). Terahertz time-domain spectroscopy. *Nature Reviews Methods Primers*, 3(1), 48. <https://doi.org/10.1038/s43586-023-00232-z>
- [18] Siegel, P. H. (2011). Terahertz pioneer: David H. Auston. *IEEE Transactions on Terahertz Science and Technology*, 1(1), 6–8. <https://doi.org/10.1109/TTHZ.2011.2151130>
- [19] Rahman, A., Rahman, A. K., & Tomalia, D. A. (2017). Engineering dendrimers to produce dendrimer dipole excitation based terahertz radiation sources suitable for spectrometry, molecular and biomedical imaging. *Nanoscale Horizons*, 2(3), 127–134. <https://doi.org/10.1039/c7nh00010c>
- [20] Zewail, A. H. (2000). Femto-chemistry: Atomic-scale dynamics of the chemical bond using ultrafast lasers. *Angewandte Chemie International Edition*, 39(15), 2586–2631. [https://doi.org/10.1002/1521-3773\(20000804\)39:15<2586::AID-ANIE2586>3.0.CO;2-O](https://doi.org/10.1002/1521-3773(20000804)39:15<2586::AID-ANIE2586>3.0.CO;2-O)
- [21] Rahman, A. (2011). Dendrimer based terahertz time-domain spectroscopy and applications in molecular characterization. *Journal of Molecular Structure*, 1006(1–3), 59–65. <https://doi.org/10.1016/j.molstruc.2011.07.004>
- [22] Hashimoto, S., Akita, K., Tanabe, T., Nakahata, H., Takeda, K., & Amano, H. (2010). Epitaxial layers of AlGaIn channel HEMTs on AlN substrates. *SEI Technical Review*, 71, 83–87.
- [23] Shi, H., Yi, A., Ding, J., Liu, X., Qin, Q., Yi, J., . . . , & Ou, X. (2023). Defect evolution in GaN thin film heterogeneously integrated with CMOS-compatible Si(100) substrate by ion-cutting technology. *Science China Information Sciences*, 66(11), 219403. <https://doi.org/10.1007/s11432-022-3668-0>
- [24] Mahfuz, M., Reza, F., Liu, X., Chu, R., Lang, M., Snure, M., . . . , & Jin, M. (2024). Microstructural changes in GaN and AlN under 950 MeV Au swift heavy ion irradiation. *Applied Physics Letters*, 124(11), 112104. <https://doi.org/10.1063/5.0189812>
- [25] Parize, J., Jarrin, T., Fées, A., Lambert, D., Jay, A., Morin, V., . . . , & Richard, N. (2024). Comparative study of collision cascades and resulting displacement damage in GaN, Si, and Ge. *IEEE Transactions on Nuclear Science*, 71(8), 1461–1469. <https://doi.org/10.1109/TNS.2024.3380674>

How to Cite: Rahman, A. (2025). GaN Lattice Damage and GaN-HEMT Metrology by Cameraless T-Ray Imaging and Time-Domain Spectroscopy. *Journal of Optics and Photonics Research*. <https://doi.org/10.47852/bonviewJOPR52025068>